# Development and Property evaluation of high entropy bulk metallic glass in RE-Al-Co system

## Current Status of Structural Materials
## – Advanced Research of Structural Materials –

2014-031814
Jinyeon Kim

# Contents

- Basic concepts of high entropy alloys and bulk metallic glasses
- History of high entropy bulk metallic glasses (HE BMGs)
- Development of novel HE BMGs in $RE^{(1)}_{18}RE^{(2)}_{18}RE^{(3)}_{20}Al_{24}Co_{20}$ alloys

1) Fragility and mechanical properties → Characteristic of BMG

2) Crystallization behaviors → Characteristic of HEA

(Stable liquid to solid during cooling & metastable liquid to solid during heating)

**" HE BMGs " ➡ Bridging between HEAs and BMGs**

# Basic concepts of high entropy alloy (HEA)

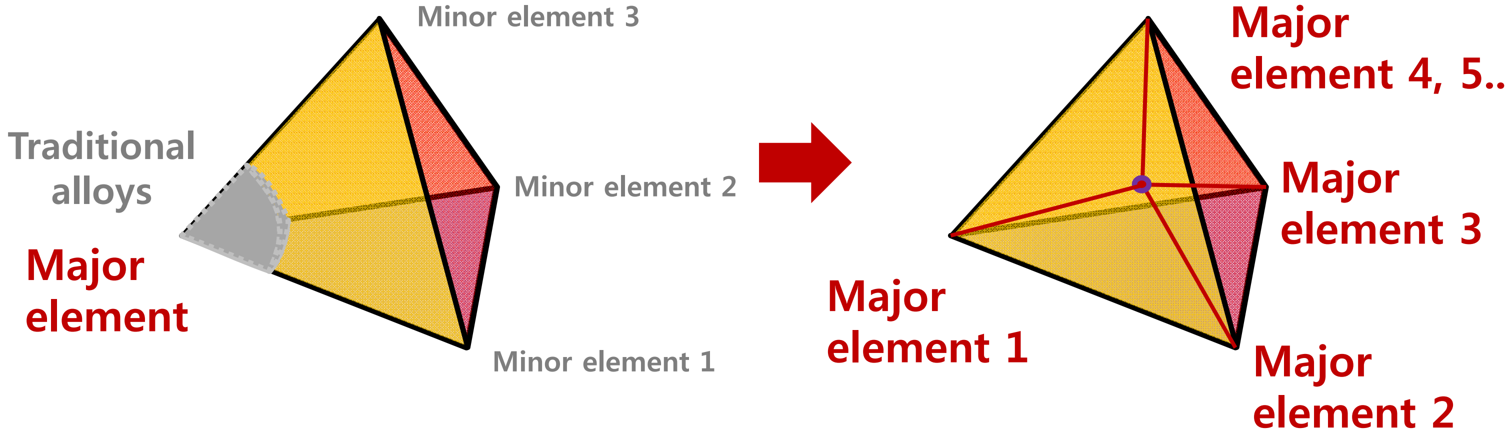


**Conventional alloy system**

**Ex) 304 steel - $Fe_{74}Cr_{18}Ni_{8}$**

**High entropy alloy system**

**Ex) $Al_{20}Co_{20}Cr_{20}Fe_{20}Ni_{20}$**

**(1) Thermodynamic : high entropy effect**

**(2) Kinetics : sluggish diffusion effect**

**(3) Structure : severe lattice distortion effect**

**(4) Property : cocktail effect**

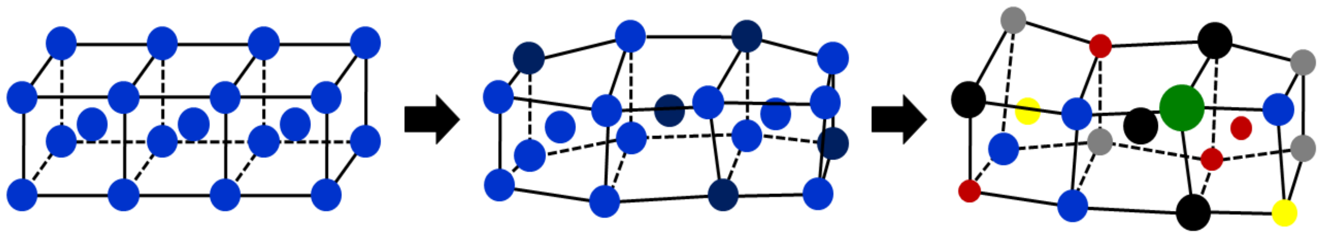

*Yong Zhang et al., Adv. Eng. Mat. P534-538, 2008*

**→ Unique dislocation behavior & High temperature stability**

# Empirical rules: high entropy alloy vs bulk metallic glass

## Multi-component system

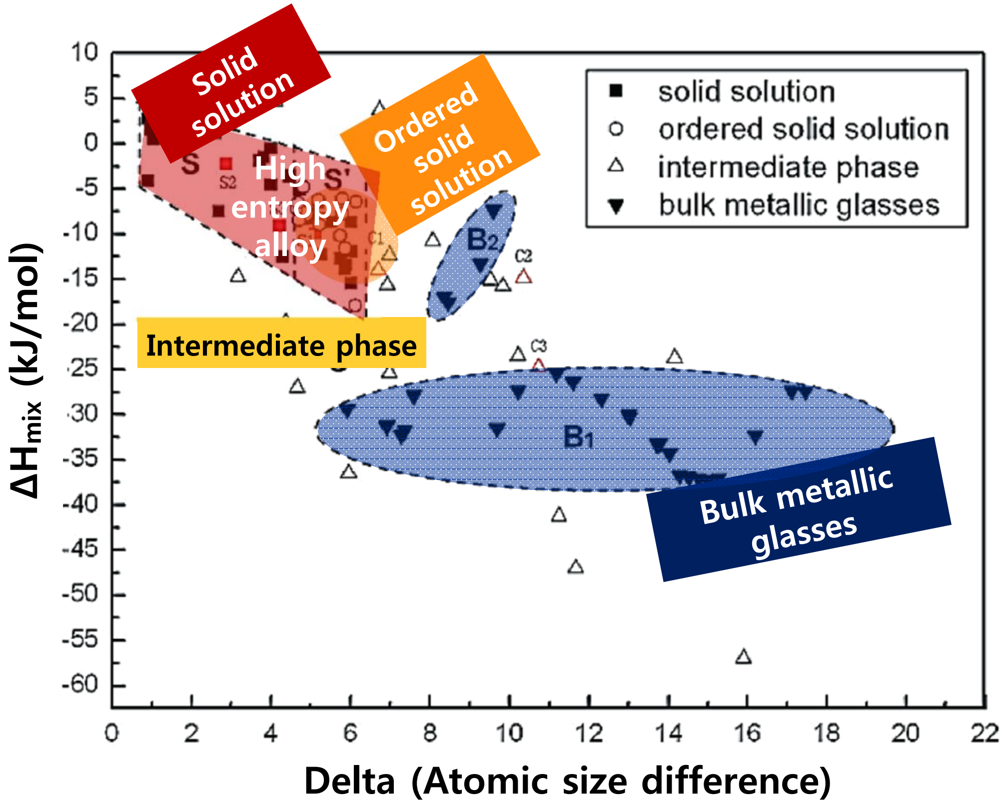


## High entropy alloy (HEA)

- Multi-component systems consisting of more than five elements
- Small difference of atomic size ratio under 12%
- Almost zero value of heats of mixing among the three main constituent elements

## Bulk metallic glass (BMG)

- multi-component systems consisting of more than three elements
- Significant difference in atomic size ratios above about 12% among the three constituent elements
- Negative heats of mixing among the three main constituent elements

➡ By linking the BMGs and HEAs, high entropy bulk metallic glass could be developed.

→ We can understand more about multi-component alloy systems.

# First report for high entropy bulk metallic glass

$Pd_{40}Cu_{30}Ni_{10}P_{20}$ + $Pd_{35}Pt_{15}Cu_{30}P_{20}$ → $Pd_{20}Pt_{20}Cu_{20}Ni_{20}P_{20}$ HE-BMG


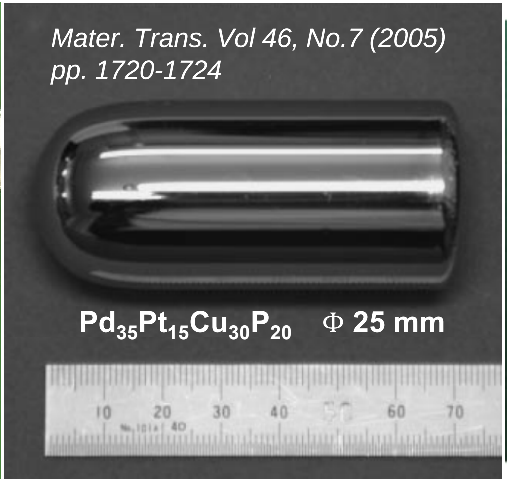


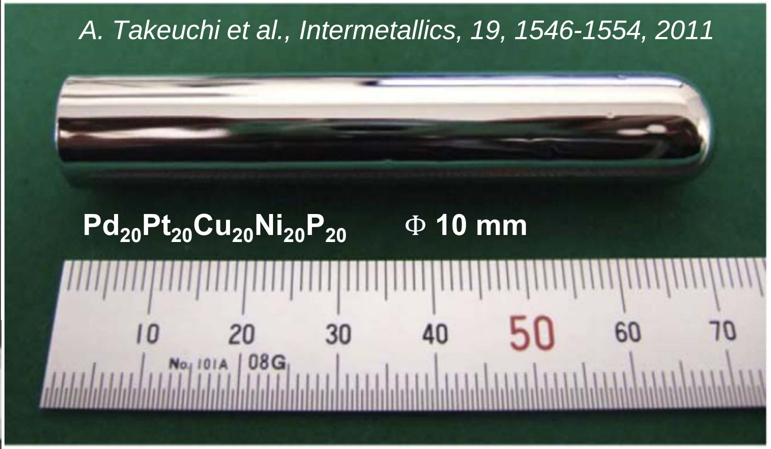


- Most BMGs have major constituent element. but, in this case, BMG has similar atomic percent of constituents.
- $Pd_{20}Pt_{20}Cu_{20}Ni_{20}P_{20}$ HE-BMG was firstly reported by combining $Pd_{40}Cu_{30}Ni_{10}P_{20}$, $Pt_{57.5}Cu_{14.7}Ni_{5.3}P_{22.5}$ ($D_{max}$=20 mm) and $Pd_{35}Pt_{15}Cu_{30}P_{20}$ BMGs with high GFA.

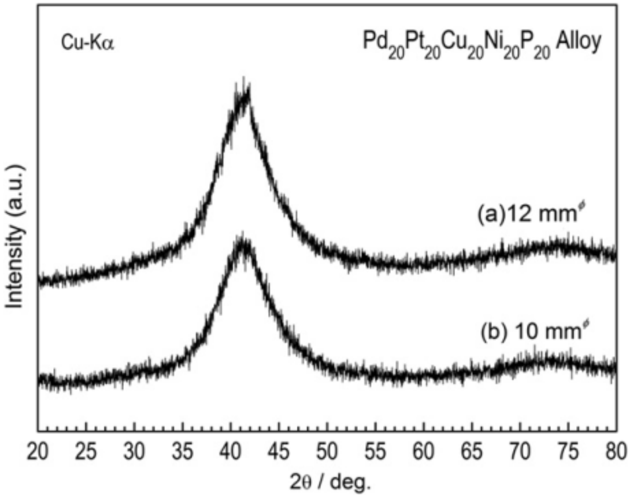

# Reported high entropy bulk metallic glasses

| Composition (at%) | $D_c$ (mm) | $T_g$ (K) | $T_x$ (K) | $\Delta T$ (K) | $\sigma_y$ (MPa) |
|---|---|---|---|---|---|
| $Ti_{20}Zr_{20}Hf_{20}Cu_{20}Ni_{20}$ | 1.5 | 658 | 711 | 53 | 1920 |
| $Zn_{20}Ca_{20}Sr_{20}Yb_{20}(Li_{0.55}Mg_{0.45})_{20}$ | 3 | 323 | 348 | 25 | <500 |
| $Sr_{20}Ca_{20}Yb_{20}Mg_{20}Zn_{20}$ | ~5 | 353 | 389 | 36 | <500 |
| $Sr_{20}Ca_{20}Yb_{20}Mg_{20}(Zn_{0.5}Cu_{0.5})_{20}$ | ~5 | 351 | 391 | 40 | <500 |
| $Er_{20}Tb_{20}Dy_{20}Ni_{20}Al_{20}$ | 2 | - | - | - | - |

→ **Development of Rare earth high entropy bulk metallic glass**

# Rare earth element based BMGs: (a) relatively high glass former

$RE_{55}Al_{25}Co_{20}$ ➡ $RE^{(1)}_{56-x}RE^{(2)}_{x}Al_{24}Co_{20}$

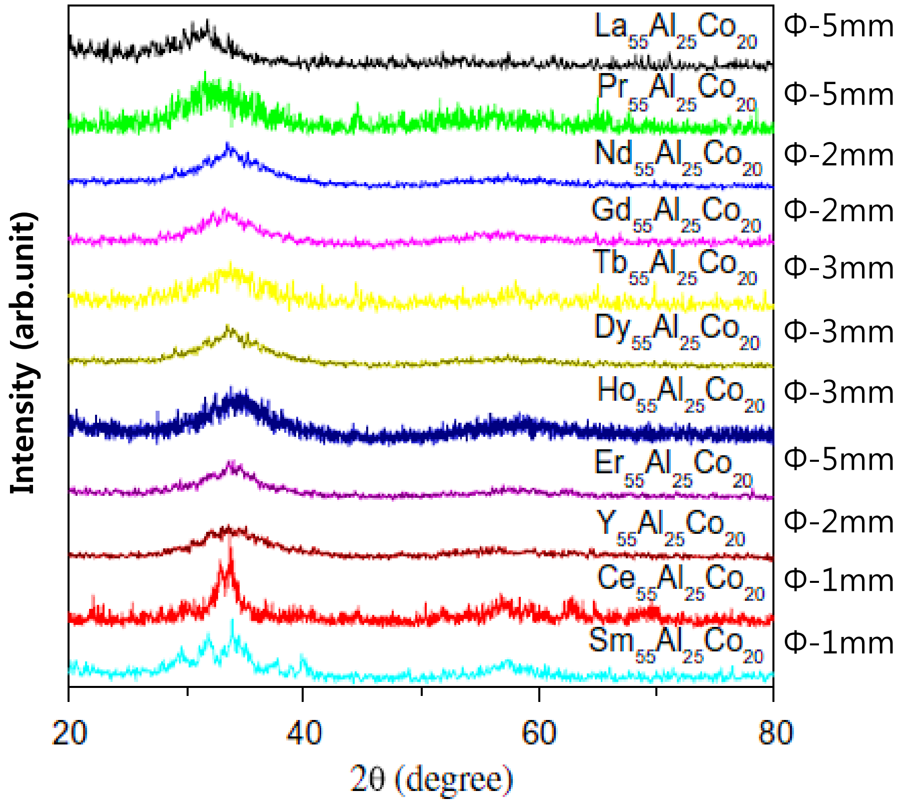


*S. Li et al., Journal of Non-Crystalline Solids 354 (2008) 1080-1088*

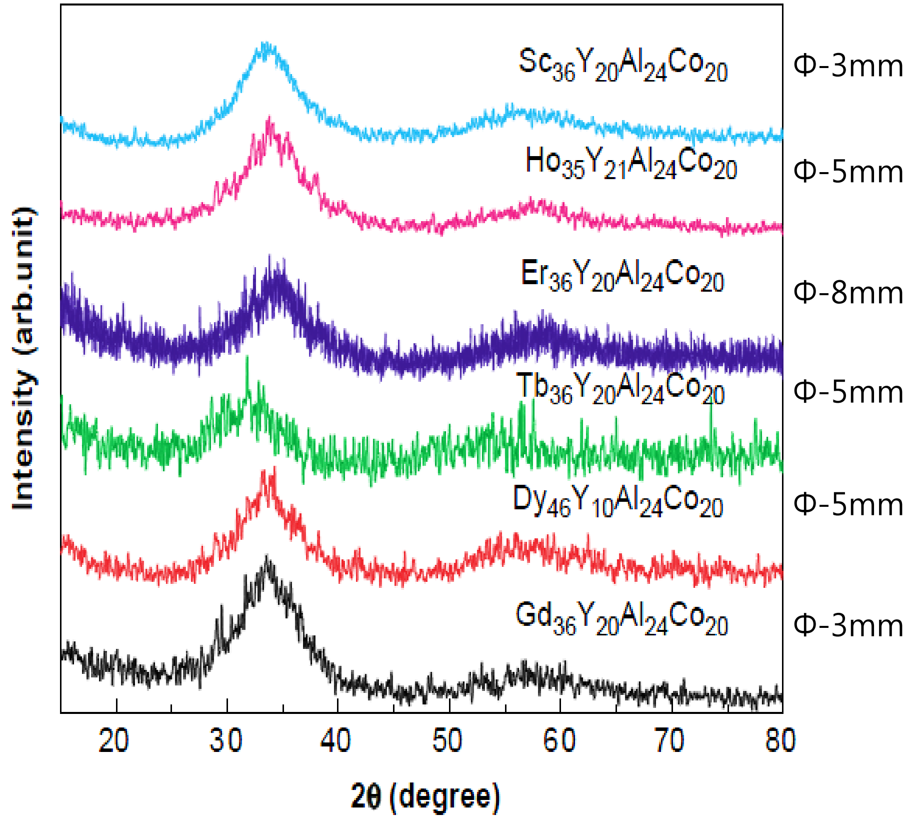


*S. Li et al., Science and technology of Advanced Materials 6 (2005) 823-827*

▶ **RE based BMGs → high GFA in simple ternary and quarternary system**

# Rare earth element based BMGs: (b) Characteristics of HE alloys

$RE_{56}Al_{24}Co_{20}$ → $RE^{(1)}_{56-x}RE^{(2)}_{x}Al_{24}Co_{20}$

*Hui Xidong et al., Chin. Sci. Bull. Vol. 56, No.36: 3978-3983, 2011*

*S. Li et al., Sci. Tech. Adv. Mater. Vol 6, p823-827, 2005*

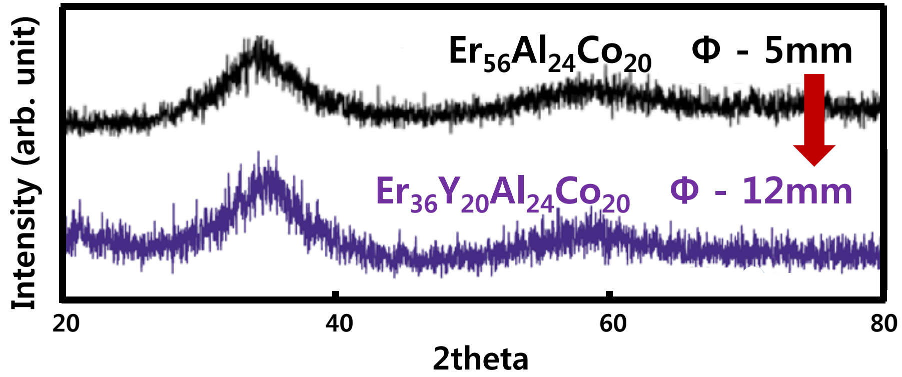


1) $\Delta H_{mix}$ ~ 0

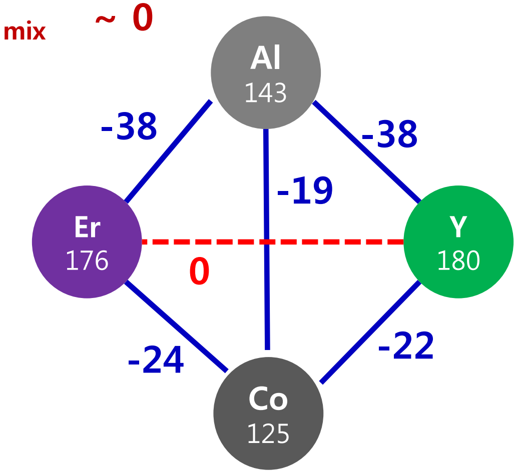


## 2) Similar properties among RE elements

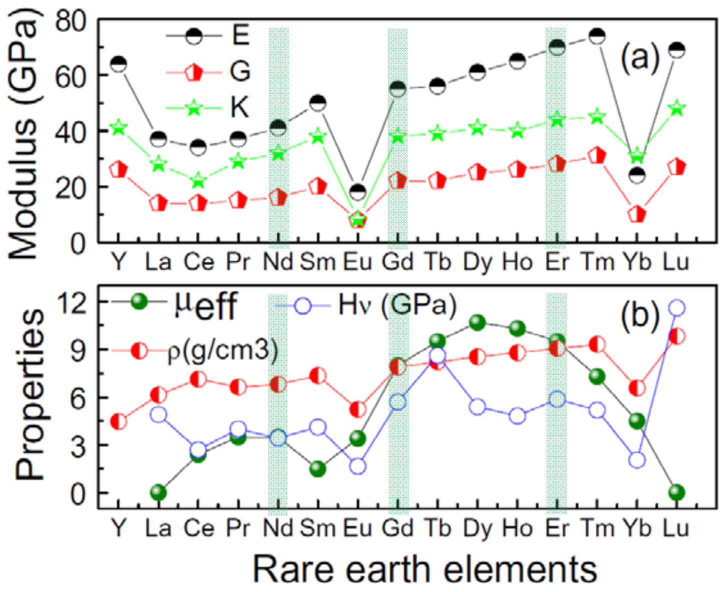


*Q. Luo et al.,* J. Non-Cryst. Solids*, 355, p759-775, 2009*

## 3) Complete solid solution among RE elements

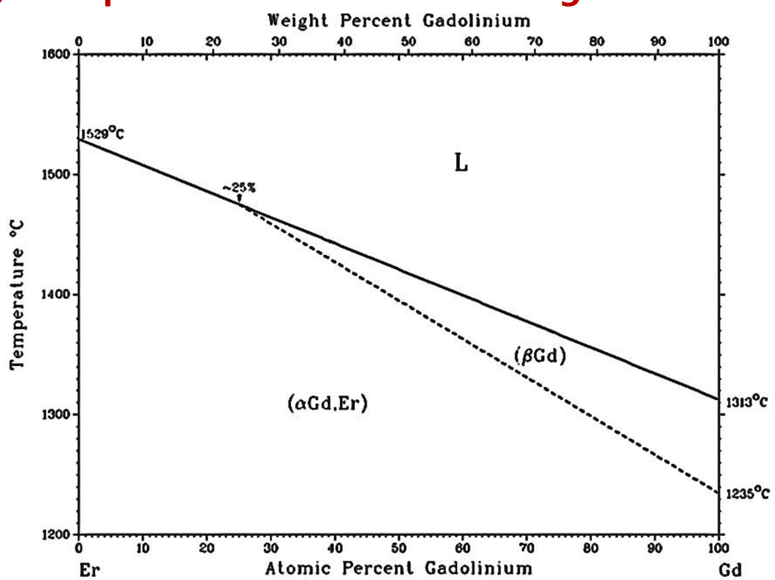

# Alloy design of high entropy bulk metallic glasses

**Rare Earth based BMGs**

$RE_{55}Al_{25}Co_{20}$

↓

$RE^{(1)}_{56-x}RE^{(2)}_{x}Al_{24}Co_{20}$

↓

**High entropy bulk metallic glass**

$RE_{55}Al_{25}Co_{20}$

↓

$RE^{(1)}_{36}RE^{(2)}_{20}Al_{24}Co_{20}$

↓

$RE^{(1)}_{18}RE^{(2)}_{18}RE^{(3)}_{20}Al_{24}Co_{20}$

▶ The number and the kinds of the rare earth elements
→ **high mixing entropy effect**

# Newly developed quarternary $RE^{(1)}_{36}RE^{(2)}_{20}Al_{24}Co_{20}$ BMGs

Unit : atomic radius [pm], heat of mixing [kJ/mol]

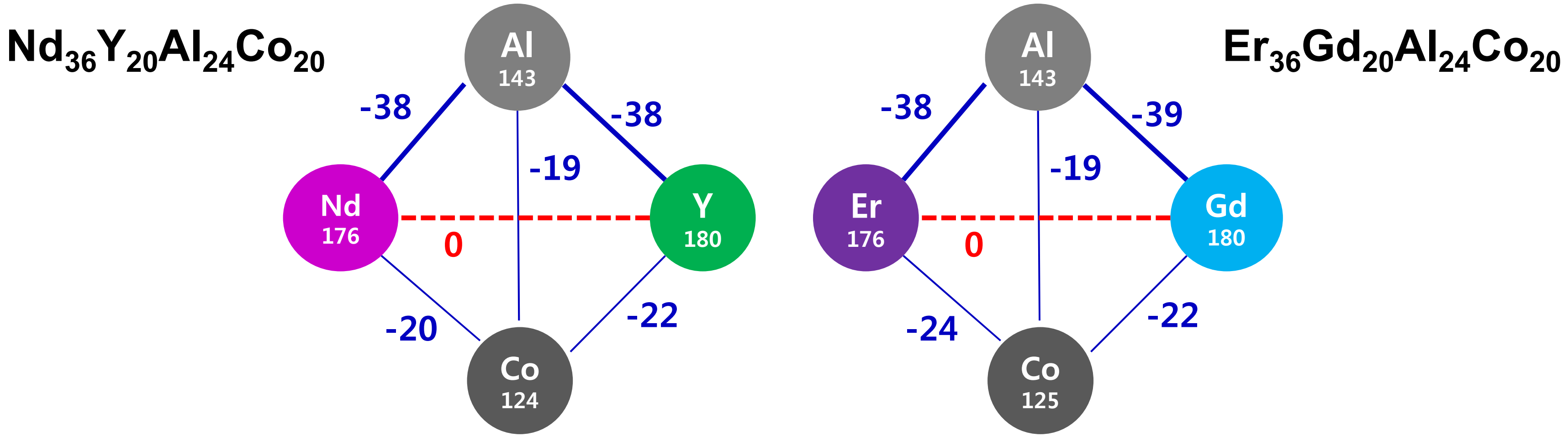


▶ Combination of a heavy rare earth elements, Al and transition metal lead to the large mismatch in atomic size and the large heat of mixing of the constituent elements → high GFA

| Composition | $T_g$ (K) | $T_x$ (K) | $\Delta T_x$ (K) | ΔH (J/g) | $D_{max}$ (mm) | |
|---|---|---|---|---|---|---|
| $Nd_{36}Y_{20}Al_{24}Co_{20}$ | 567 | 634 | 67 | -92 | ≥2 | Present work |
| $Er_{36}Gd_{20}Al_{24}Co_{20}$ | 639 | 677 | 38 | -72 | ≥2 | Present work |

## Extension of alloy design for $RE^1RE^2RE^3$-Al-TM HE BMG system

# Alloy design : $RE^{(1)}_{18}RE^{(2)}_{18}RE^{(3)}_{20}Al_{24}Co_{20}$ HE BMGs

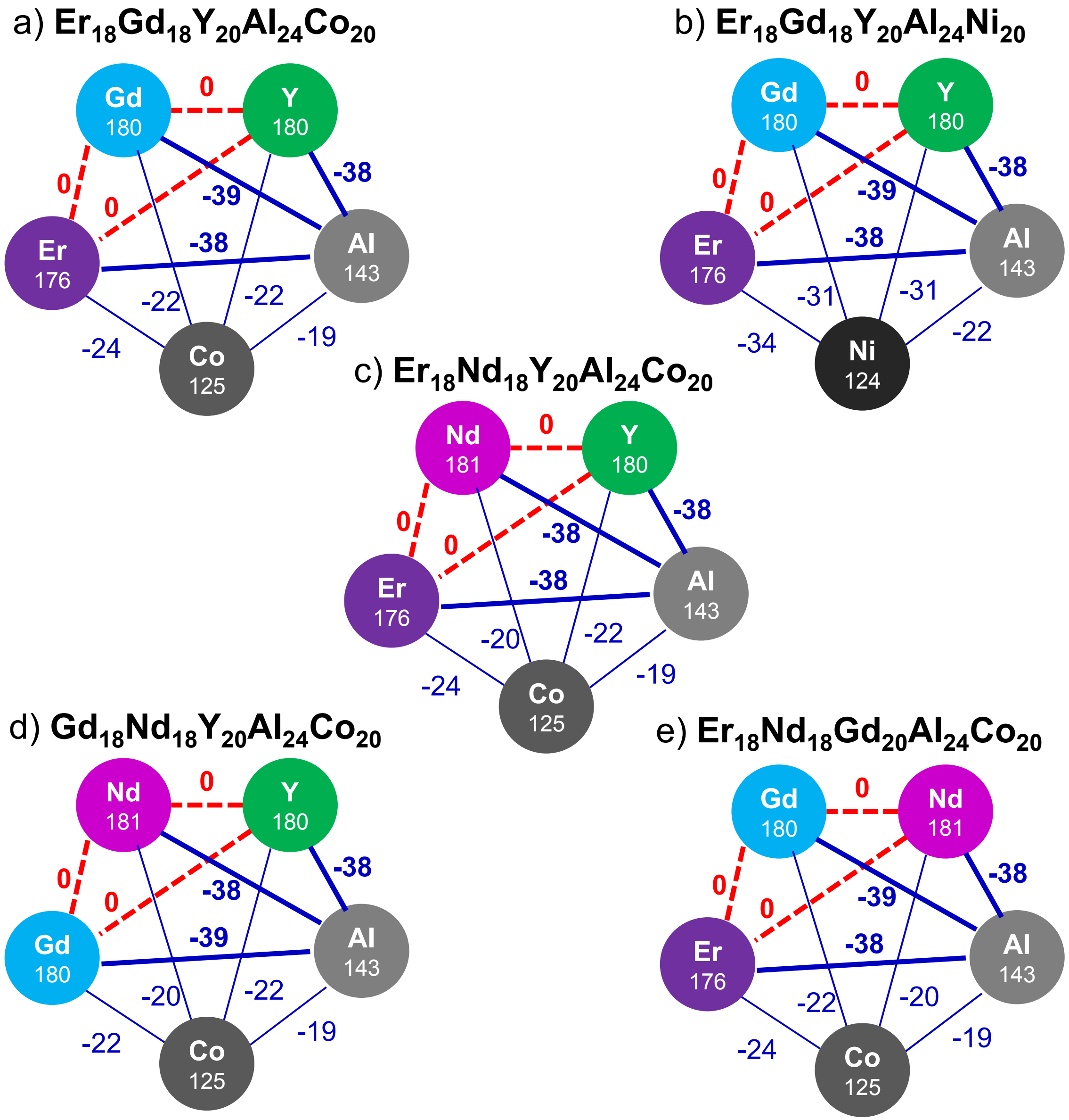


Unit : atomic radius [pm], heat of mixing [kJ/mol]

# Glass formation in $RE^{(1)}_{18}RE^{(2)}_{18}RE^{(3)}_{20}Al_{24}Co_{20}$ HE samples

**Er & Gd & Nd & Y : Select 3 elements + Al + Co & Ni : Select 1 element**

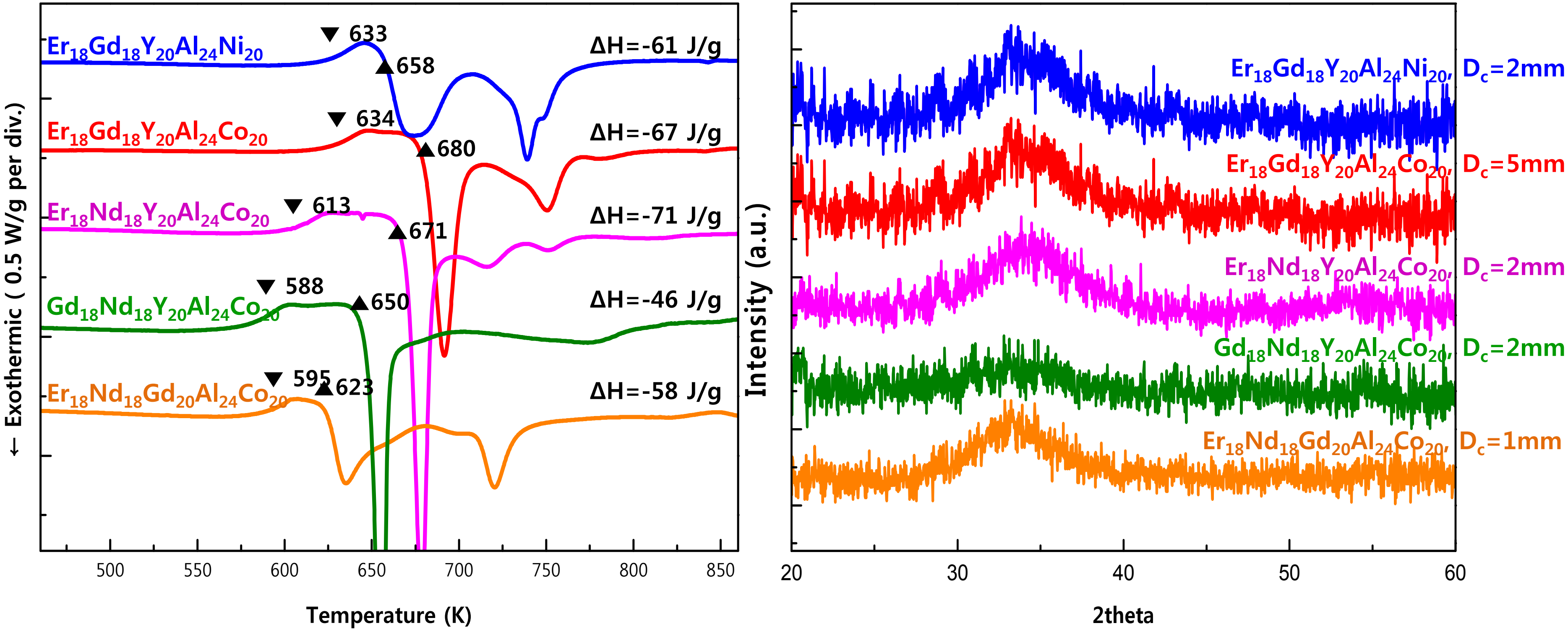


- **Above five HE compositions show clear supercooled liquid region before crystallization in DSC traces and broad diffuse peaks in XRD patterns of ribbons and bulk samples.**

→ **Fully amorphous ribbons and bulk samples are fabricated in above five RE-based high entropy compositions.**

# Development of novel $RE^{(1)}_{18}RE^{(2)}_{18}RE^{(3)}_{20}Al_{24}Co_{20}$ HE BMGs

## $Er_{18}Gd_{18}Y_{20}Al_{24}Co_{20}$ high entropy bulk metallic glass: $D_{max}$ ≥5 mm

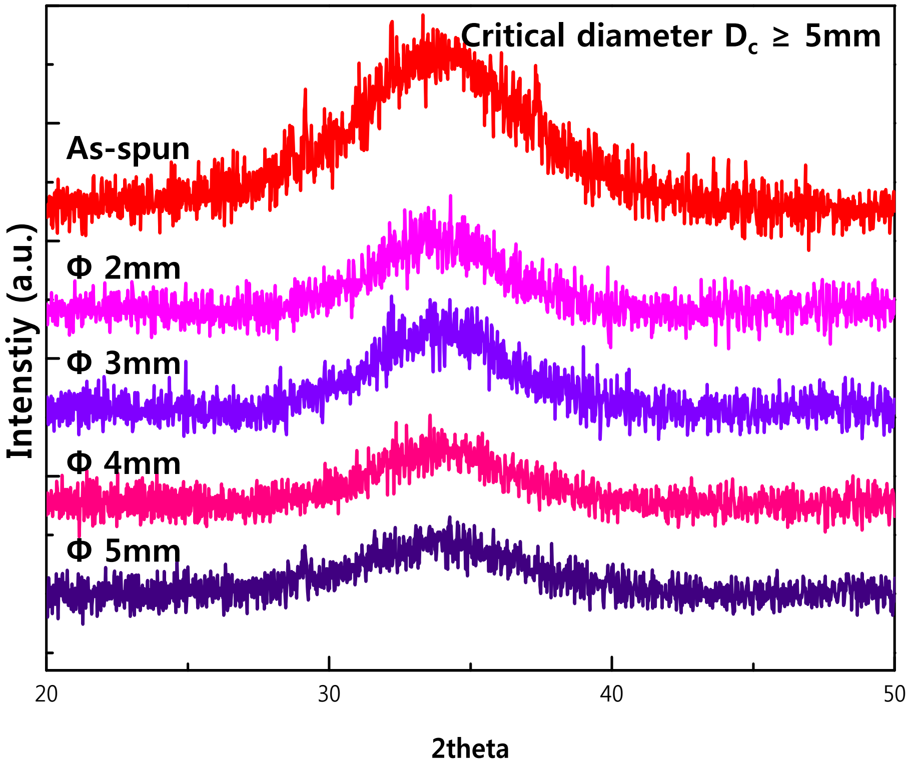


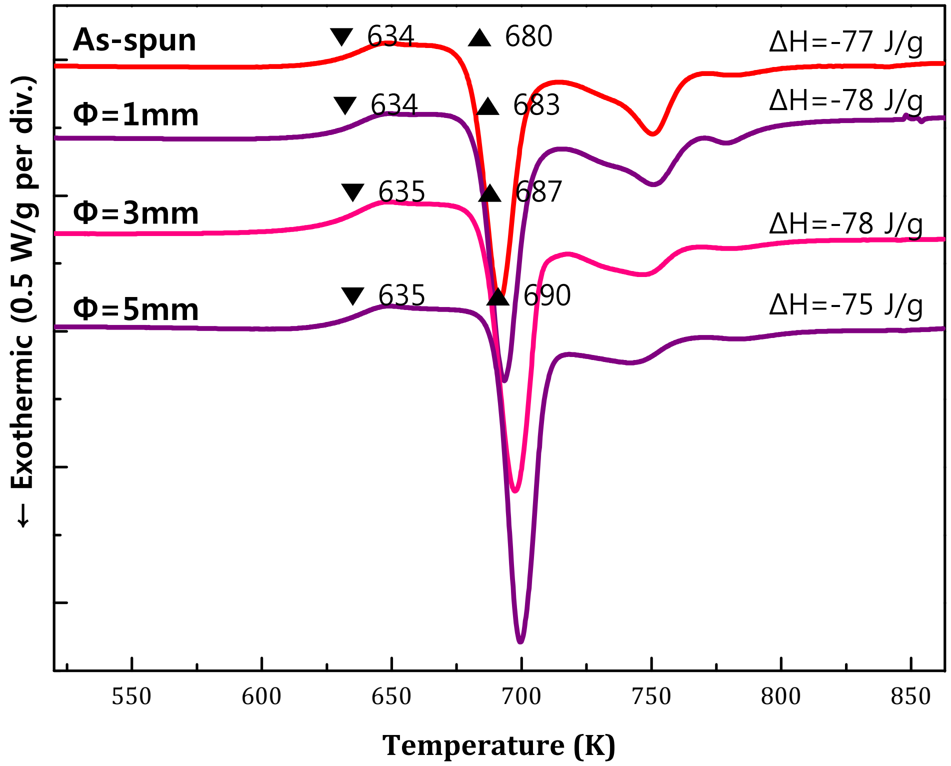


- Fully amorphous bulk samples up to 5 mm in diameter can be fabricated by suction casting method in $Er_{18}Gd_{18}Y_{20}Al_{24}Co_{20}$ high entropy alloy compositions.

# HR-TEM image for $Er_{18}Gd_{18}Y_{20}Al_{24}Co_{20}$ 5mm bulk sample

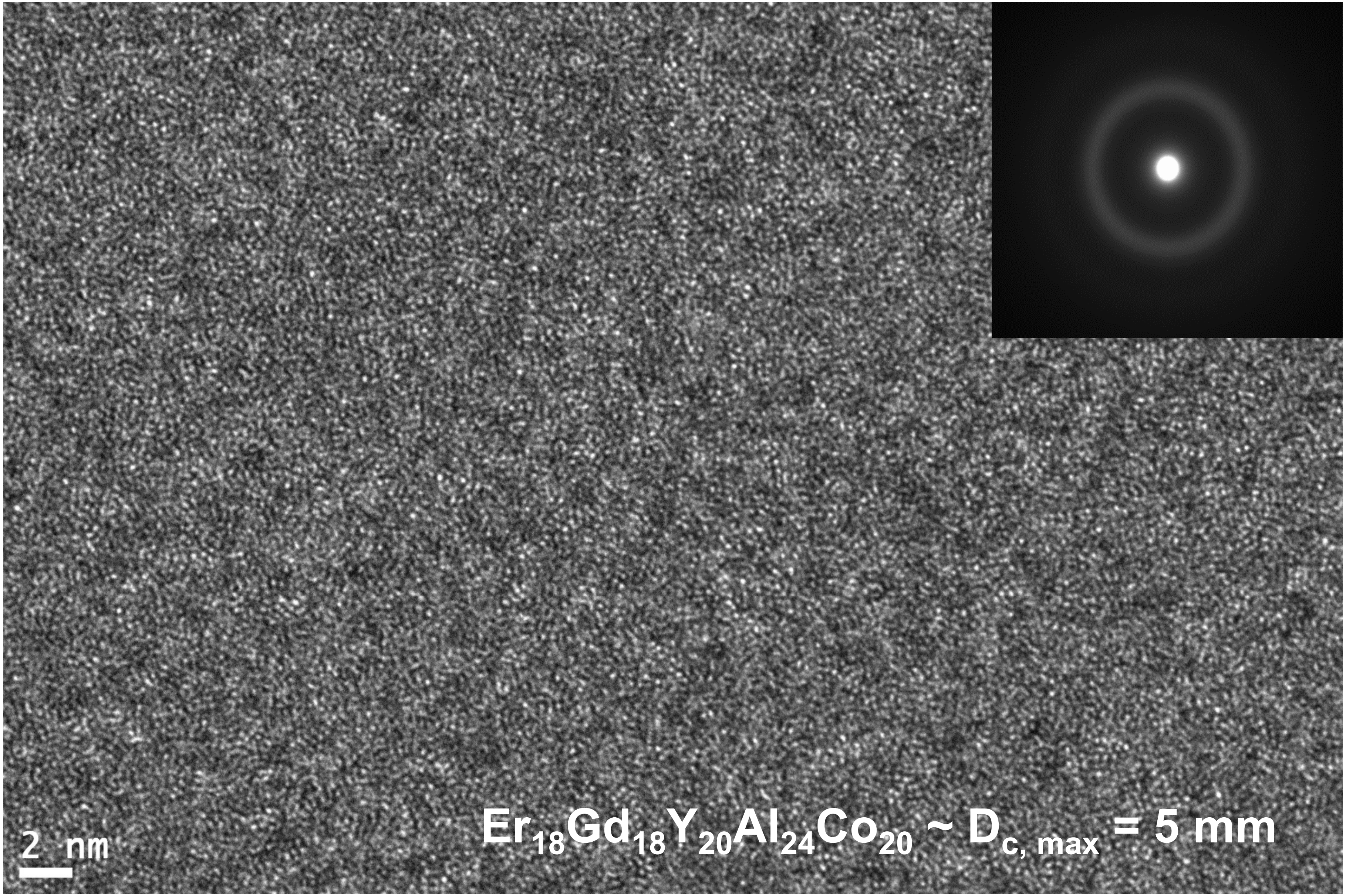

# Newly developed $RE^{(1)}_{18}RE^{(2)}_{18}RE^{(3)}_{20}Al_{24}Co_{20}$ HE BMGs

| Composition | $T_g$ (K) | $T_x$ (K) | $T_l$ (K) | $T_{rg}$ | γ | $D_{max}$ (mm) |
|---|---|---|---|---|---|---|
| $Er_{18}Gd_{18}Y_{20}Al_{24}Ni_{20}$ | 633 | 656 | 1021 | 0.620 | 0.397 | 2 |
| $Er_{18}Gd_{18}Y_{20}Al_{24}Co_{20}$ | 634 | 680 | 1031 | 0.615 | 0.408 | 5 |
| $Er_{18}Nd_{18}Y_{20}Al_{24}Co_{20}$ | 613 | 671 | 988 | 0.621 | 0.419 | 2 |
| $Gd_{18}Nd_{18}Y_{20}Al_{24}Co_{20}$ | 588 | 651 | 1004 | 0.586 | 0.409 | 1 |
| $Er_{18}Nd_{18}Gd_{20}Al_{24}Co_{20}$ | 595 | 624 | 962 | 0.619 | 0.401 | 1 |

- Five RE-based HE BMGs are newly developed in this study.
- GFA parameters ($T_{rg}$ and γ) do not show a linear correlation with the GFA of developed RE-base HE BMGs.

# Criterion for glass formation

$T_{rg}$ parameter $= T_g / T_m$

: ability to avoid crystallization during cooling

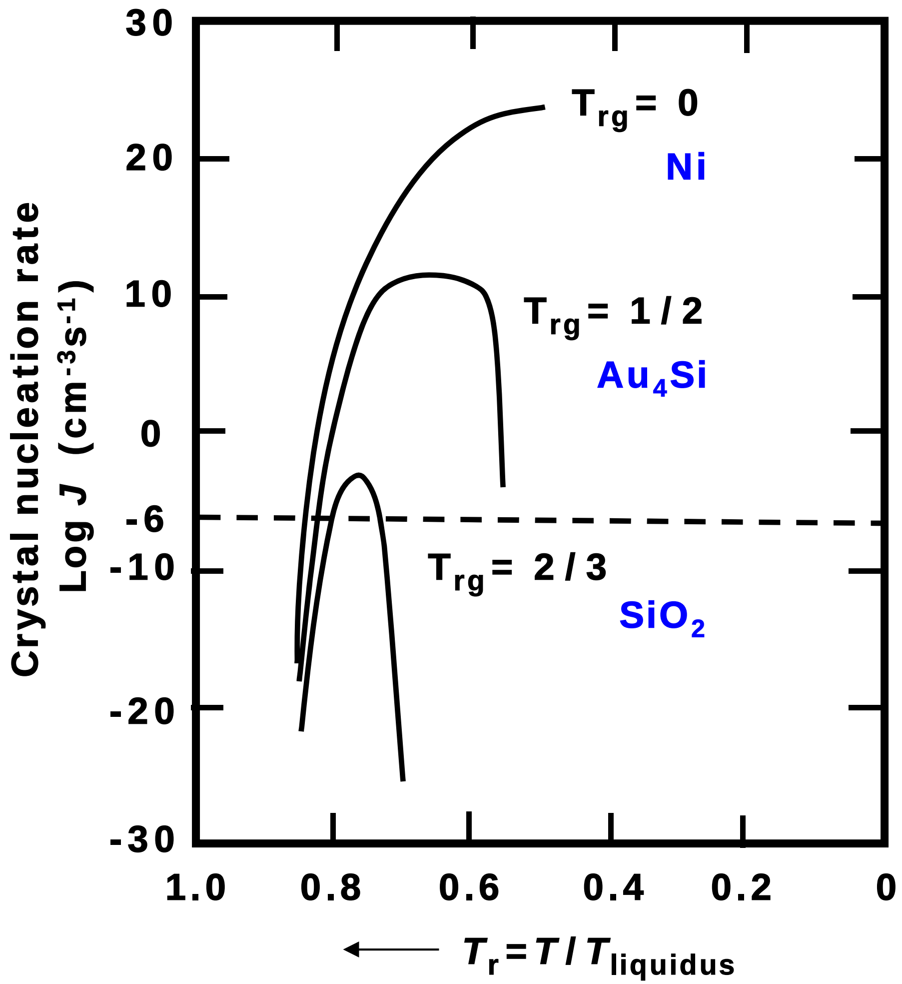


$T_{rgNi} < T_{rgAu4Si} < T_{rgSiO2}$

$R_{Ni} > R_{Au4Si} > R_{SiO2}$

*Turnbull, 1959* ff.

# Criterion for glass formation

$$\gamma \propto T_x \left[ \frac{1}{2(T_g + T_l)} \right] \propto \frac{T_x}{T_g + T_l}$$

$\gamma_a < \gamma_b \Rightarrow R_a > R_b$

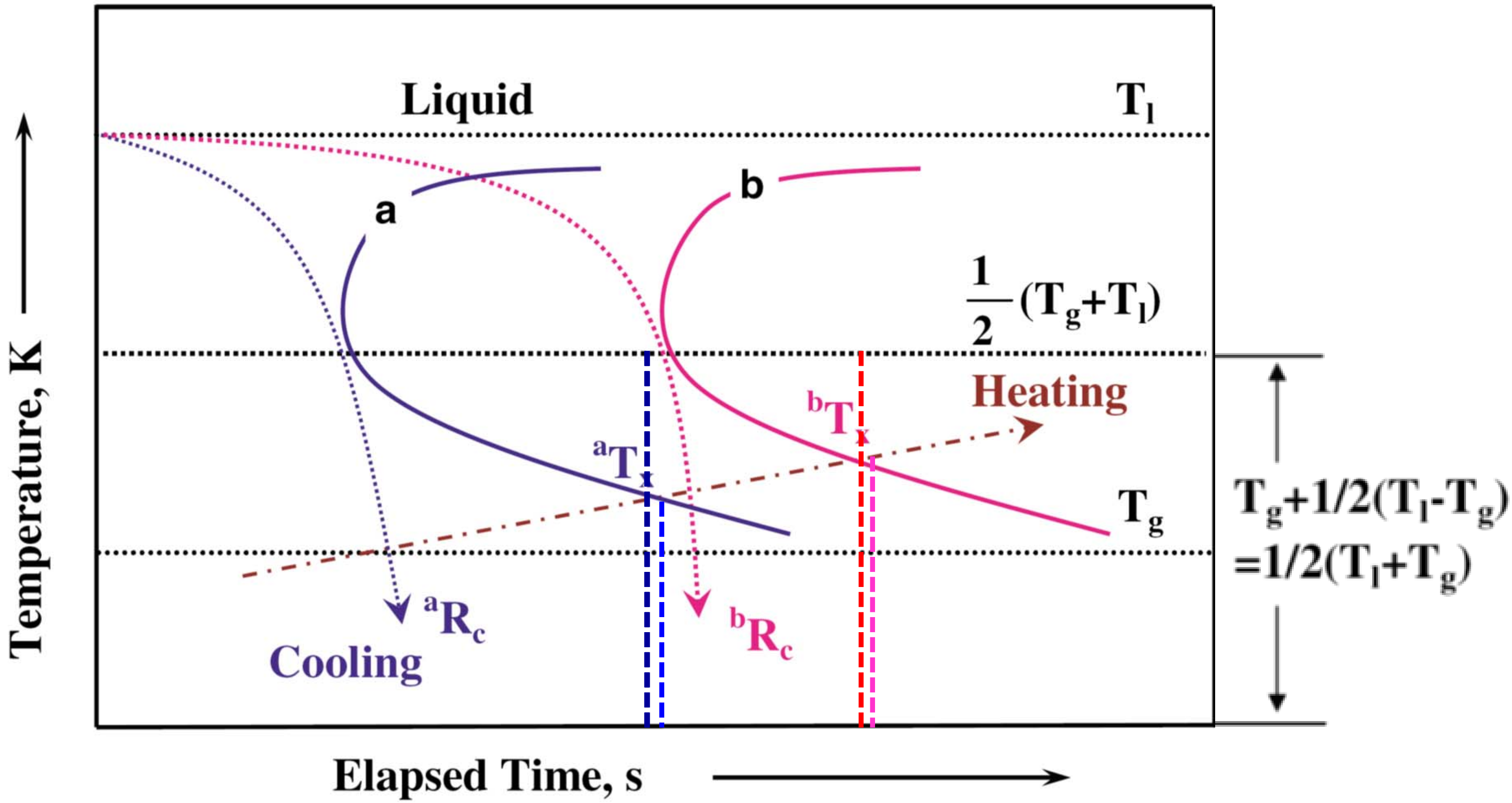


*Z.P.Lu, C.T.Liu, Acta Mater. 50 (2002) 3501*

# Newly developed $RE^{(1)}_{18}RE^{(2)}_{18}RE^{(3)}_{20}Al_{24}Co_{20}$ HE BMGs

| Composition | $T_g$ (K) | $T_x$ (K) | $T_l$ (K) | $T_{rg}$ (≥ 0.6) | γ (≥ 0.35) | $D_{max}$ (mm) |
|---|---|---|---|---|---|---|
| $Er_{18}Gd_{18}Y_{20}Al_{24}Ni_{20}$ | 633 | 656 | 1021 | 0.620 | 0.397 | 2 |
| $Er_{18}Gd_{18}Y_{20}Al_{24}Co_{20}$ | 634 | 680 | 1031 | 0.615 | 0.408 | 5 |
| $Er_{18}Nd_{18}Y_{20}Al_{24}Co_{20}$ | 613 | 671 | 988 | 0.621 | 0.419 | 2 |
| $Gd_{18}Nd_{18}Y_{20}Al_{24}Co_{20}$ | 588 | 651 | 1004 | 0.586 | 0.409 | 1 |
| $Er_{18}Nd_{18}Gd_{20}Al_{24}Co_{20}$ | 595 | 624 | 962 | 0.619 | 0.401 | 1 |

- Five RE-based HE BMGs are newly developed in this study.
- GFA parameters ($T_{rg}$ and γ) do not show a linear correlation with the GFA of developed RE-base HE BMGs.

# Property evaluation of RE based HE-BMG

1. Mechanical property
   - Nano-indentation
   - Fragility

2. Phase transformation
   - From stable liquid to solid ; Solidification
   - From meta-stable liquid to solid ; Crystallization

# I. Fragility and Mechanical properties : Characteristic of BMG

# Fragility

- **Fragility ~ extensively use to figure out liquid dynamics and glass properties corresponding to "frozen" liquid state**

## < Classification of glass >

***Strong network glass*** **: Arrhenius behavior**

$$\eta = \eta_0 \exp[\frac{E_a}{RT}]$$

***Fragile network glass*** **: Vogel-Fulcher relation**

$$\eta = \eta_0 \exp[\frac{B}{T - T_0}]$$

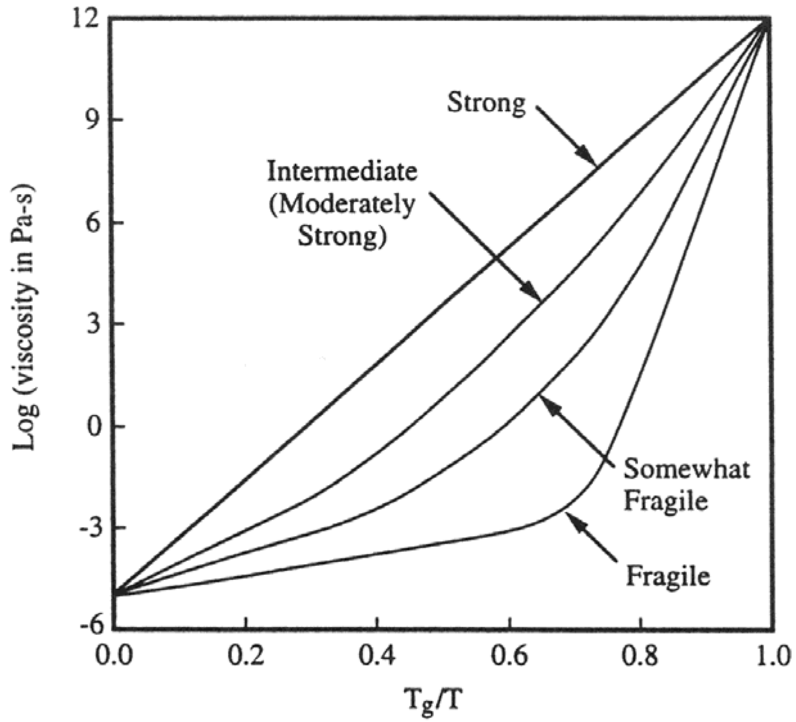


## < Quantification of Fragility >

$$m = \left.\frac{d \log \eta(T)}{d(T_{g,n}/T)}\right|_{T=T_{g,n}} = \left.\frac{d \log \tau(T)}{d(T_g/T)}\right|_{T=T_g}$$

**Slope of the logarithm of viscosity, η (or structural relaxation time, τ ) at** $T_g$

# Correlation between fragility and elastic properties in BMGs

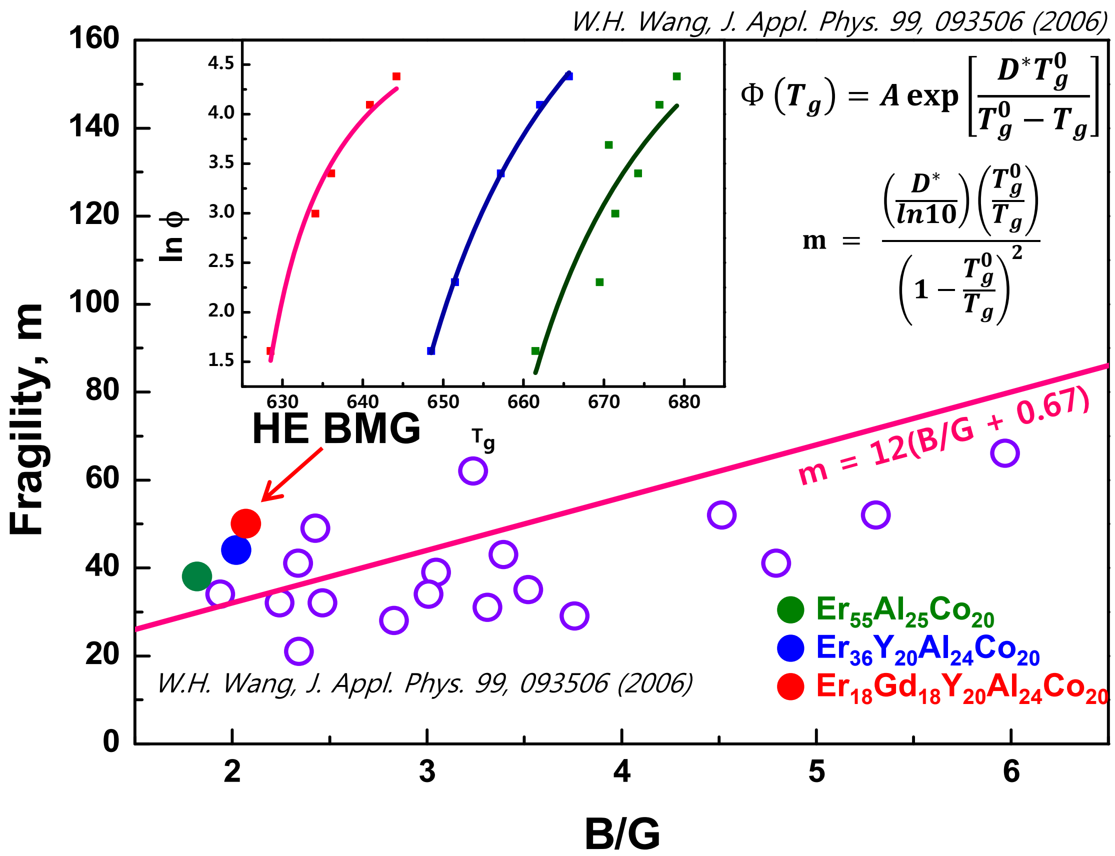


1 $Zr_{41}Ti_{14}Cu_{12.5}Ni_{10}Be_{22.5}$ [a]
2 $Zr_{46.75}Ti_{8.25}Cu_{7.5}Ni_{10}Be_{27.5}$ [a]
3 $Zr_{65}Al_{10}Ni_{10}Cu_{15}$ [a]
4 $Cu_{50}Zr_{50}$ [b]
5 $(Cu_{50}Zr_{50})_{92}Al_8$ [b]
6 $(Cu_{50}Zr_{50})_{92}Al_7Gd_1$ [b]
7 $Pd_{39.1}Ni_{10.1}Cu_{29.9}P_{20.9}$ [a]
8 $Pd_{77.5}Si_{16.5}Cu_6$ [c]
9 $Pd_{40}Ni_{40}P_{20}$ [d]
10 $Pt_{60}Ni_{15}P_{25}$ [e]
11 $Ce_{70}Al_{10}Ni_{10}Cu_{10}$ [f]
12 $Pr_{60}Al_{10}Ni_{10}Cu_{20}$ [g]
13 $Gd_{40}Y_{16}Al_{24}Co_{20}$ [b]
14 $La_{55}Al_{25}Cu_{10}Ni_5Co_5$ [a]
15 $Nd_{60}Al_{10}Fe_{20}Co_{10}$ [h]
16 $Mg_{65}Cu_{25}Gd_{10}$ [h]
17 $Fe_{70}B_5C_5Si_3Al_5Ga_2P_{10}$ [i]
18 $Ho_{39}Al_{25}Co_{20}Y_{16}$

| | B/G | Fragility, m |
|---|---|---|
| $Er_{56}Al_{24}Co_{20}$ | 1.82 | 38 |
| $Er_{36}Y_{20}Al_{24}Co_{20}$ | 2.02 | 44.07 |
| $Er_{18}Gd_{18}Y_{20}Al_{24}Co_{20}$ | 2.07 | 50.02 |

| Thermodynamic fragility | Kinetic fragility |
|---|---|
| $m_T = \left[\frac{d(\Delta S_g/\Delta S)}{d(T_g/T)}\right]_{T=T_g}$ | $m = \left[\frac{d\log\eta}{d(T_g/T)}\right]_{T=T_g}$ |

# Mechanical properties for RE-based (HE) BMGs

## Relatively low yield strength of HE BMG than RE BMGs: "Softening behavior"

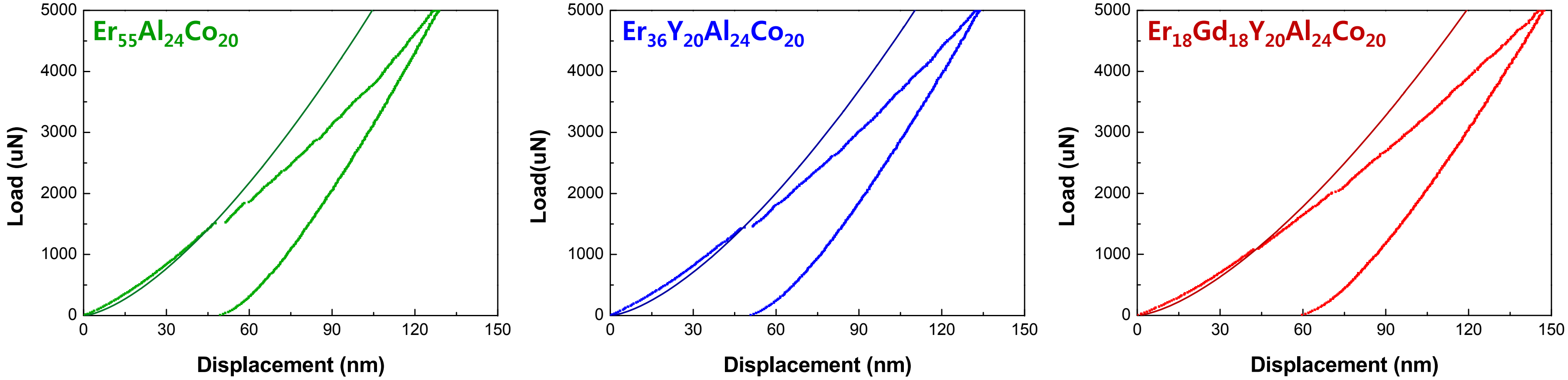


Unloading/loading rate : 1mN/sec, Maximum Load : 5mN, Conical tip (r=2um), as-spun samples

Strain rate : $10^{-4}$ /sec, 1mm rod samples

| | Nano-indentation | | | Compression test | |
|---|---|---|---|---|---|
| | Reduced elastic modulus [GPa] | Nano-hardness [GPa] | Yield strength [Gpa] | Elastic modulus [GPa] | Yield strength [GPa] |
| $Er_{55}Al_{25}Co_{20}$ [Er55] | 73.31±6.6 | 5.50±0.5 | 2.18±0.2 | 79.79 | 1.60 |
| $Er_{36}Y_{20}Al_{24}Co_{20}$ [Er36] | 73.0±9.0 | 5.37±0.3 | 2.17±0.2 | 72.94 | 1.46 |
| $Er_{18}Gd_{18}Y_{20}Al_{24}Co_{20}$ [Er18] | 65.18±4.2 | 4.81±0.2 | 2.0±0.2 | 65.71 | 1.24 |

**' Fragility ➡ Characteristic of BMG '**

# II. Crystallization behavior: Characteristic of HEA

1) Stable liquid to crystalline phase during cooling: Solidification

2) Metastable liquid to crystalline phase during heating: Crystallization

# Property evaluation of $Er_{18}Gd_{18}Y_{20}Al_{24}Co_{20}$ HE BMG

1. **Mechanical property**
   - **Nanoindentation / compression test**
   - **Fragility**

2. **Thermal property (phase transformation)**
   - **Cooling : stable liq. → solid ; Electrostatic levitation**
   - **Heating : supercooled liq. → solid ; DSC & TEM**

# Electrostatic levitation in KRISS

**Containerless equipment: close to homogeneous nucleation**

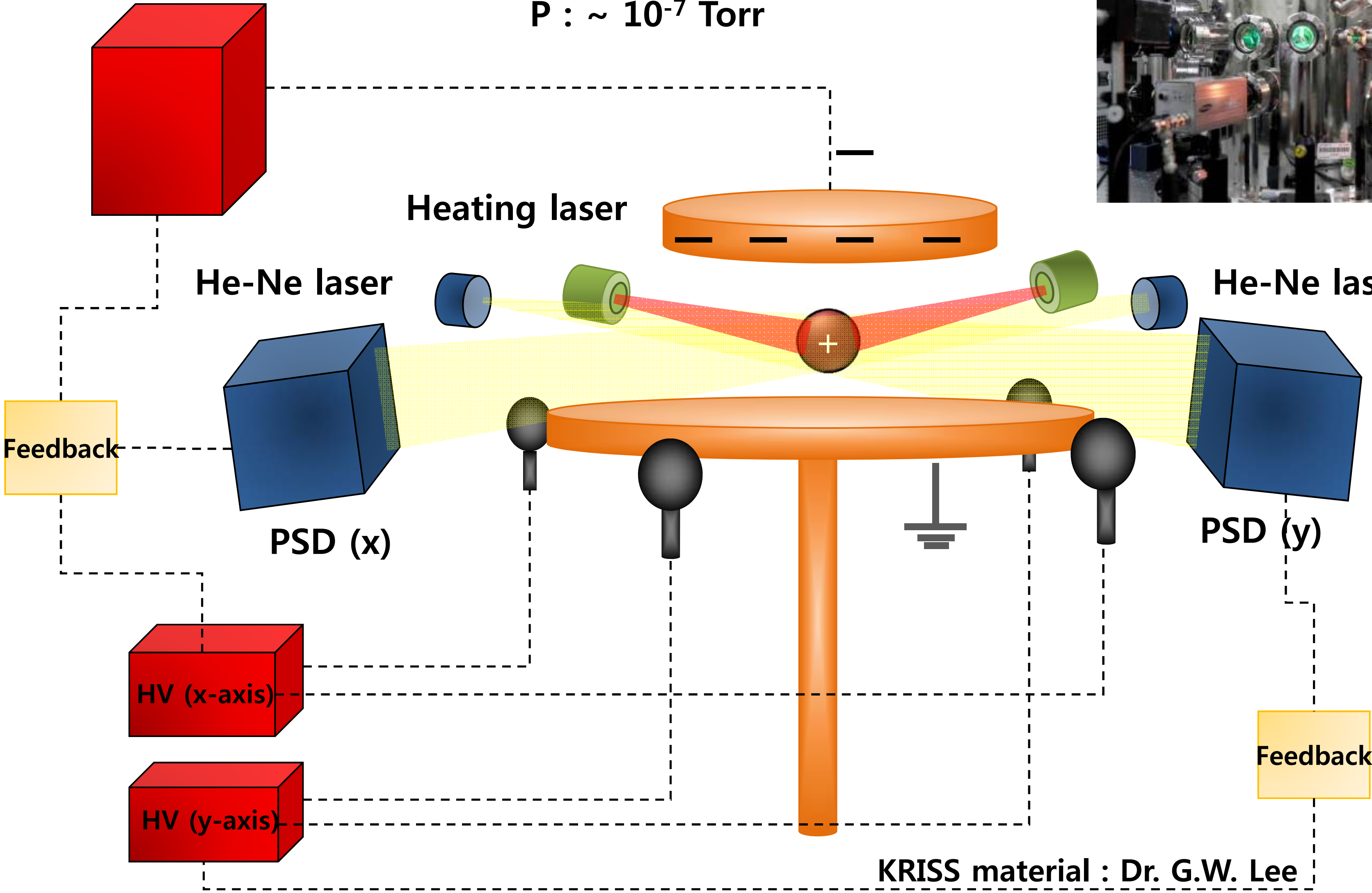


KRISS material : Dr. G.W. Lee

# Cooling curve for Er(-Gd-Y)-Al-Co BMG & HE BMG system

## 1) Phase transformation from stable liquid to solid : cooling

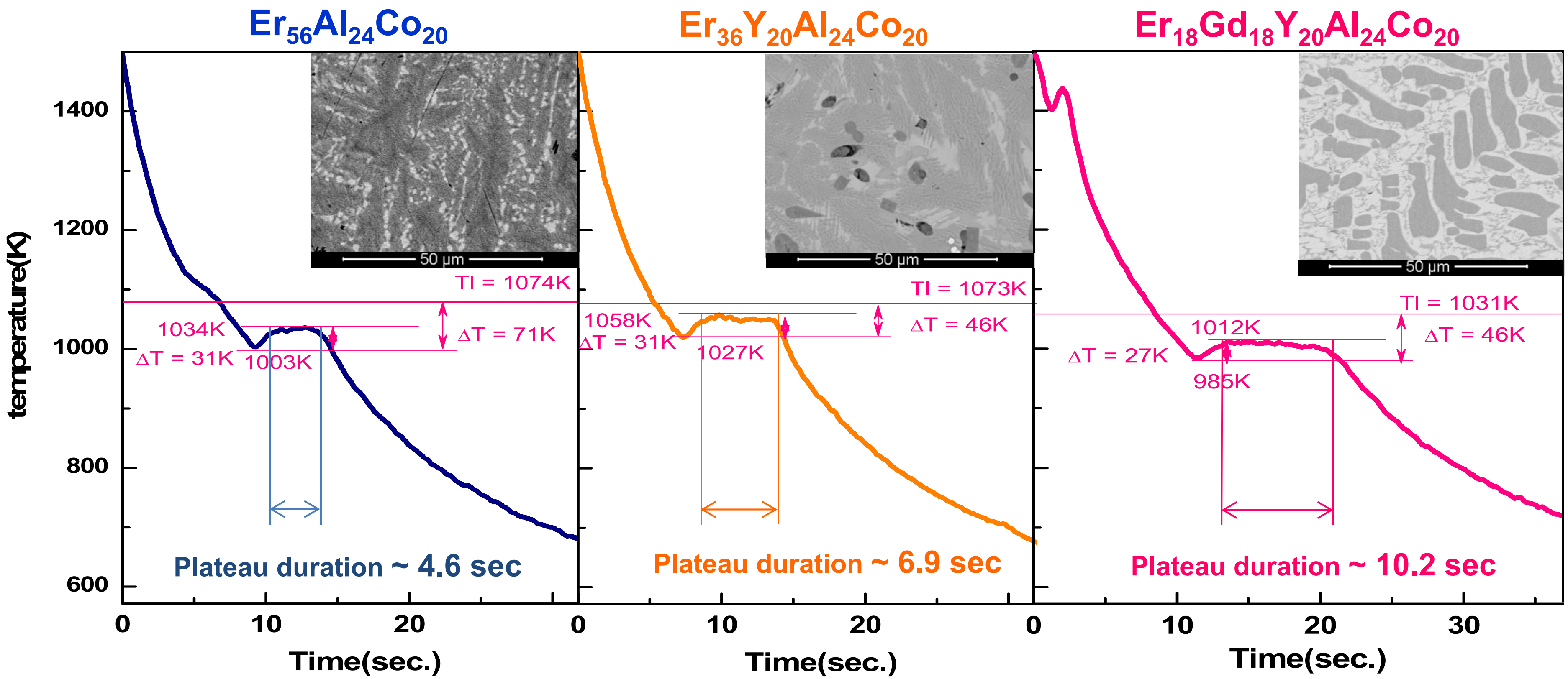


**HE BMG: Relatively longer time to growth**

**‘ Sluggish diffusion behavior in stable liquid ➡ characteristic of HEA ’**

# Property evaluation of $Er_{18}Gd_{18}Y_{20}Al_{24}Co_{20}$ HE BMG

1. **Mechanical property**
   - **Nanoindentation / compression test**
   - **Fragility**

2. **Thermal property (phase transformation)**
   - **Cooling : stable liq. → solid ; Electrostatic levitation**
   - **Heating : supercooled liq. → solid ; DSC & TEM**

# TEM image of $Er_{18}Gd_{18}Y_{20}Al_{24}Co_{20}$ HE BMG

## 2) Phase transformation from metastable liquid to solid : heating

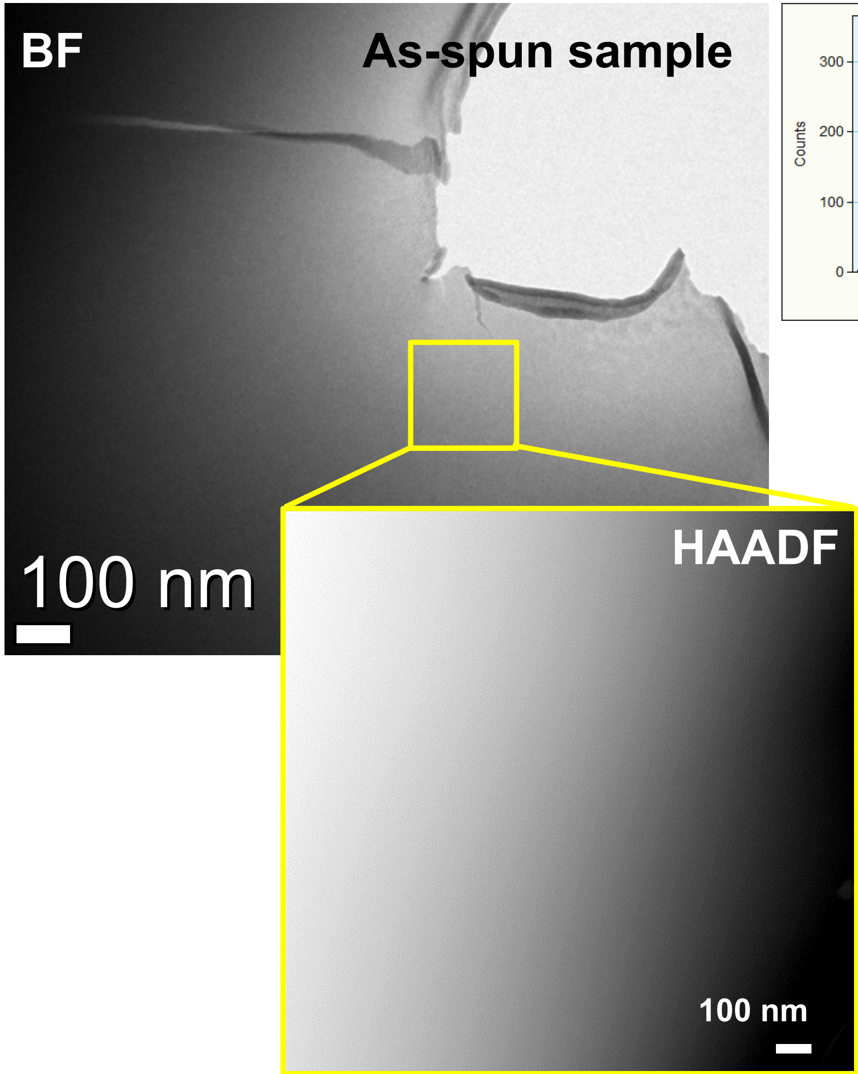


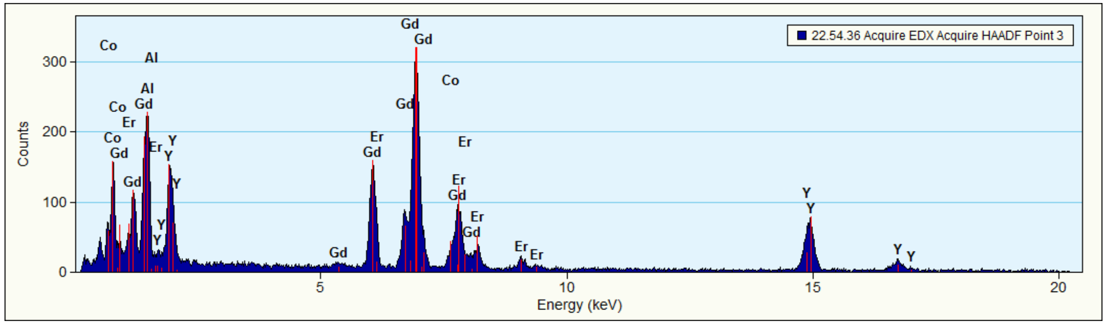


| Element | Atomic % |
|---|---|
| Al (K) | 21.58 |
| Co (K) | 18.95 |
| Y (K) | 17.2 |
| Gd (L) | 18.36 |
| Er (L) | 23.88 |
| RE | 59.44 |

**No composition contrast**

➡ **Fully amorphous state**

# Crystallization behavior of $Er_{18}Gd_{18}Y_{20}Al_{24}Co_{20}$ HE-BMG

## 2) Phase transformation from metastable liquid to solid : heating

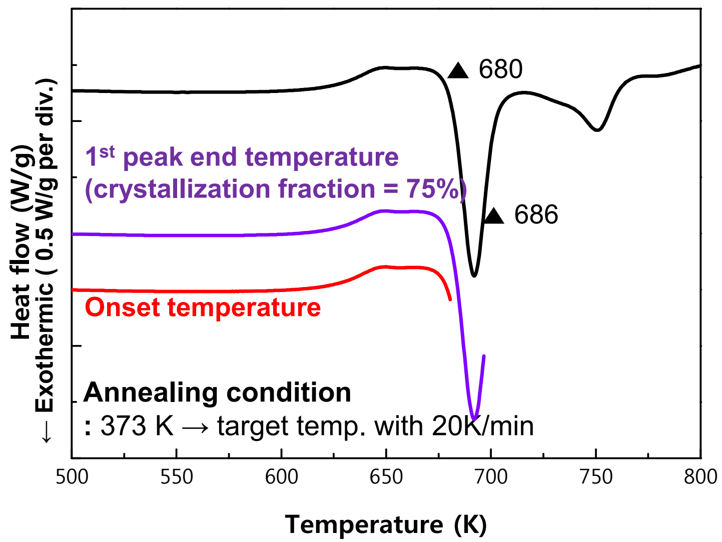


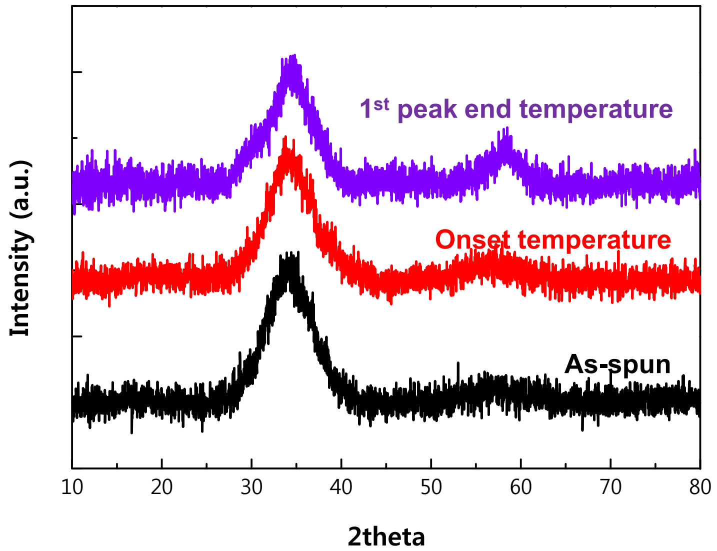


# AlY precipitation of HE BMG annealed at 1st peak mid temp. (686 K)

## 2) Phase transformation from metastable liquid to solid : heating

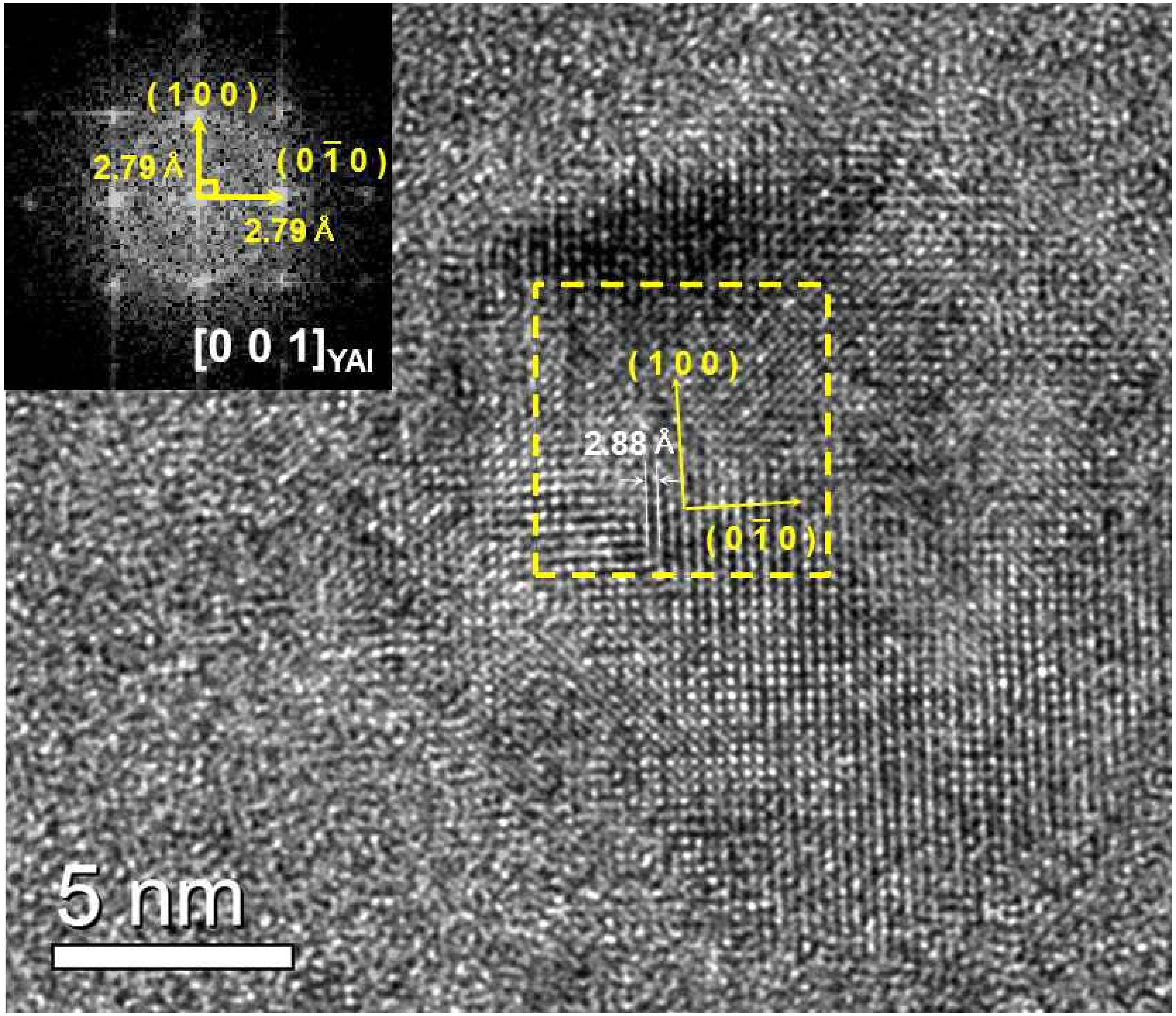

# $Er_{18}Gd_{18}Y_{20}Al_{24}Co_{20}$ HE BMG annealed to onset temp. of $T_x$ (680K)

## 2) Phase transformation from metastable liquid to solid : heating

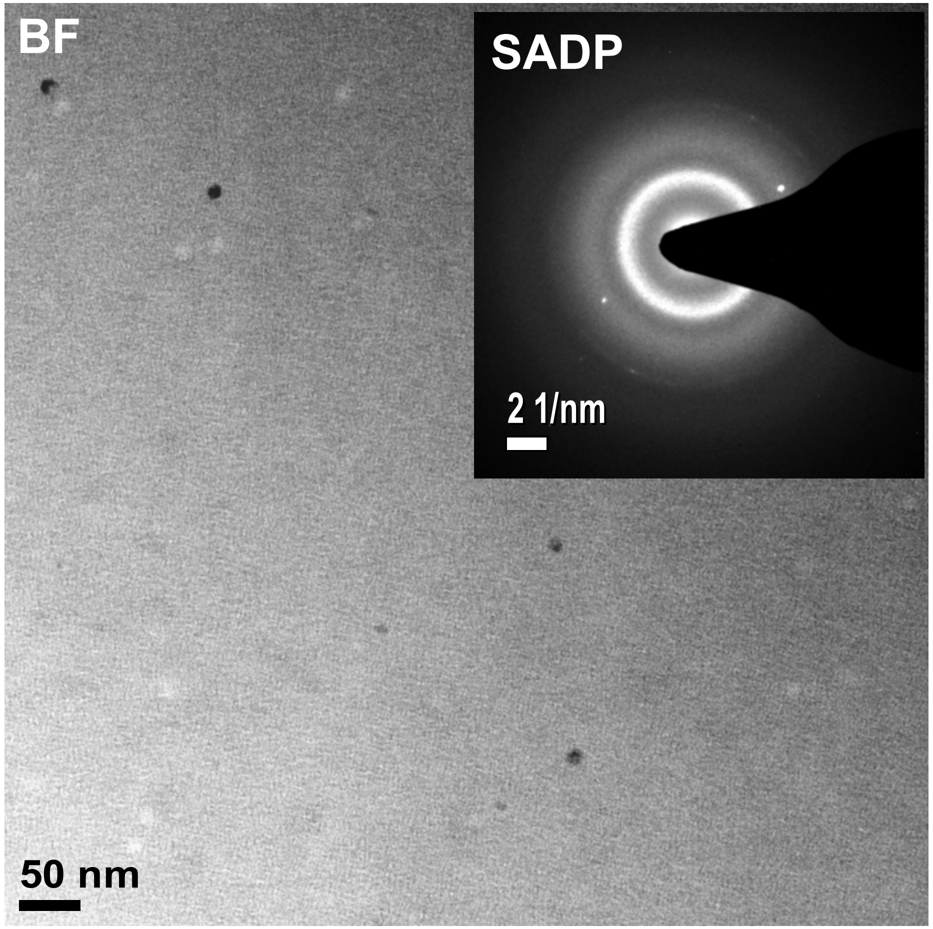


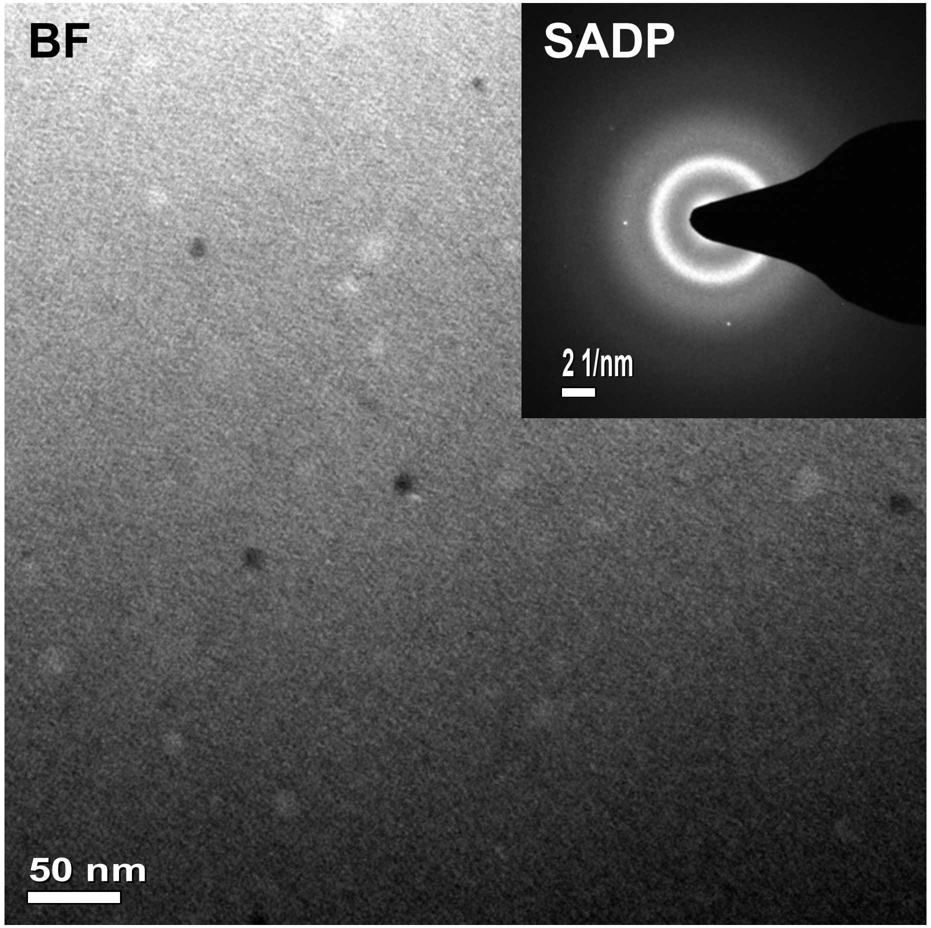


**‘ Sluggish diffusion behavior in SCL ➡ Slow growth rate ’**

# SAXS experiment in PALS

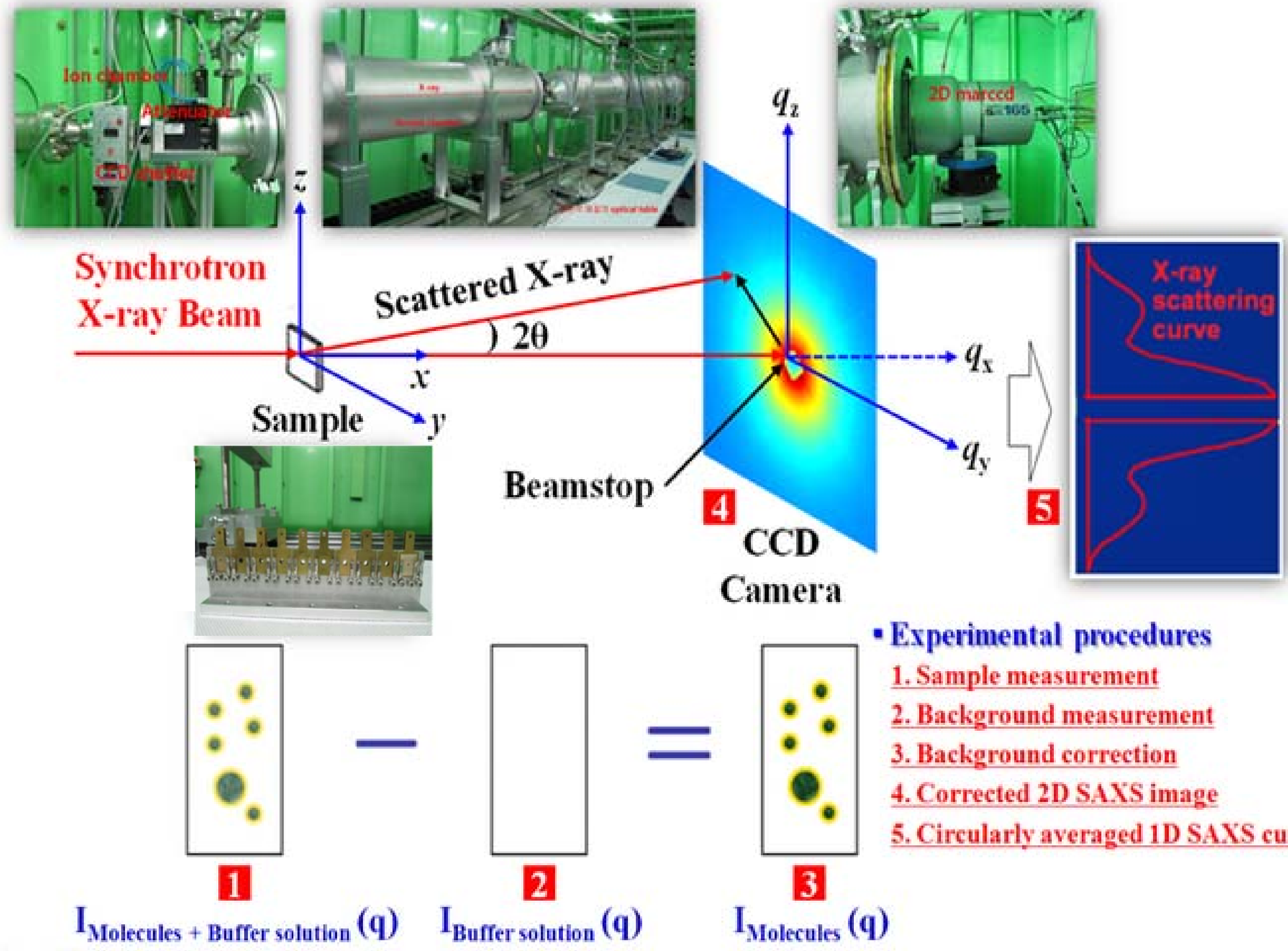


- Experimental procedures
  1. Sample measurement
  2. Background measurement
  3. Background correction
  4. Corrected 2D SAXS image
  5. Circularly averaged 1D SAXS curve

# SAXS patterns and Size distribution of crystalline phases

- $Er_{18}Gd_{18}Y_{20}Al_{24}Co_{20}$ ribbon samples annealed at different T

**Nanoscale precipitation starts at ~ 680 K**

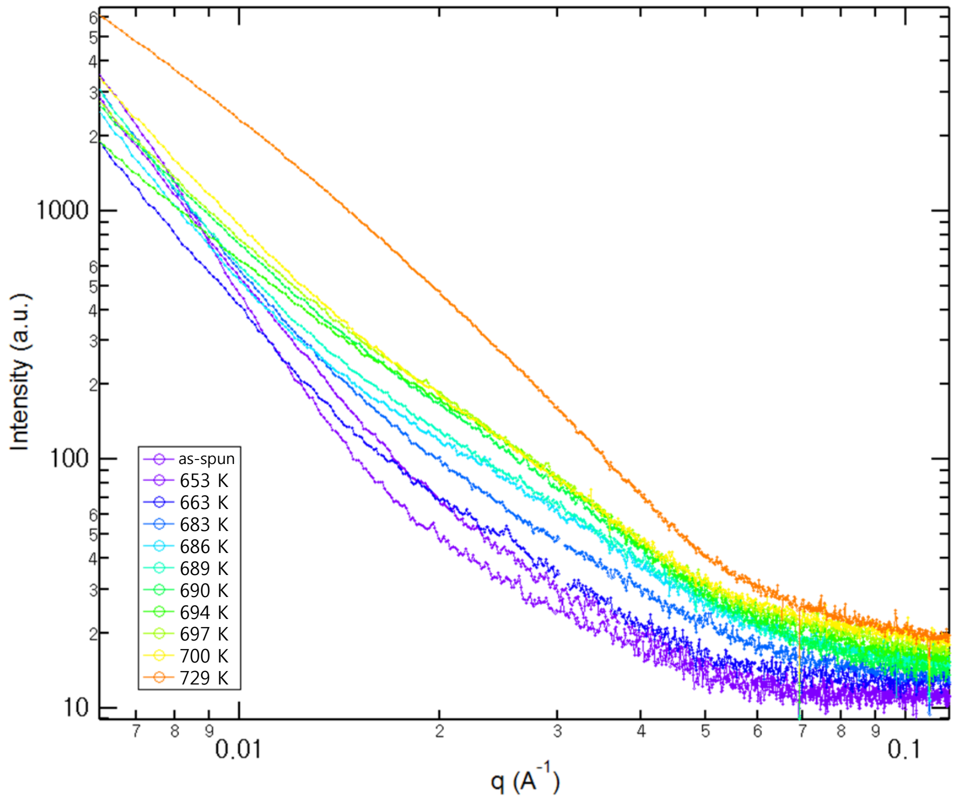


**Average size of precipitate: 10 nm → 15 nm**

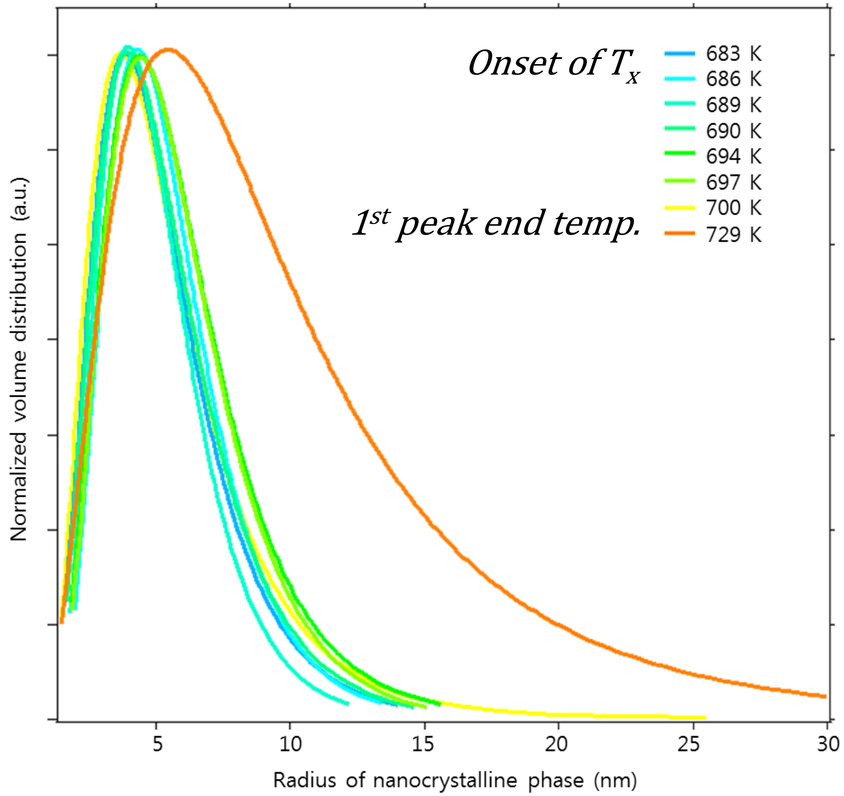


**' Sluggish diffusion behavior in SCL ➡ Slow growth rate '**

# Summary

1. Novel high entropy BMGs can be developed in $RE^{(1)}_{18}RE^{(2)}_{18}RE^{(3)}_{20}Al_{24}Co_{20}$ alloys.

   In particular, $Er_{18}Gd_{18}Y_{20}Al_{24}Co_{20}$ HE BMG can be fabricated over 5 mm in dia.

| Composition | $T_g$ (K) | $T_x$ (K) | $T_l$ (K) | $T_{rg}$ | γ | $D_{max}$ (mm) |
|---|---|---|---|---|---|---|
| $Er_{18}Gd_{18}Y_{20}Al_{24}Ni_{20}$ | 633 | 656 | 1021 | 0.620 | 0.397 | 2 |
| $Er_{18}Gd_{18}Y_{20}Al_{24}Co_{20}$ | 634 | 680 | 1031 | 0.615 | 0.408 | 5 |
| $Er_{18}Nd_{18}Y_{20}Al_{24}Co_{20}$ | 613 | 671 | 988 | 0.621 | 0.419 | 2 |
| $Gd_{18}Nd_{18}Y_{20}Al_{24}Co_{20}$ | 588 | 651 | 1004 | 0.586 | 0.409 | 1 |
| $Er_{18}Nd_{18}Gd_{20}Al_{24}Co_{20}$ | 595 | 624 | 962 | 0.619 | 0.401 | 1 |

2. Characteristic of bulk metallic glass : "more fragile" and "Softening behavior"
   - $Er_{18}Gd_{18}Y_{20}Al_{24}Co_{20}$ HE BMG is more fragile glass former and, as a consequence, has relatively low elastic modulus, hardness and yield strength.

3. Characteristic of high entropy alloy : " Sluggish diffusion behavior "
   - Phase transformation from stable liquid to solid during cooling
     : longer plateau → relatively long time to growth during solidification
   - Phase transformation from metastable liquid to solid during heating
     : average size of precipitates during 1st crystallization ~ 10 nm – relatively slow growth rate

# Summary

**' HE BMGs ' ➡ Bridging between HEAs and BMGs**

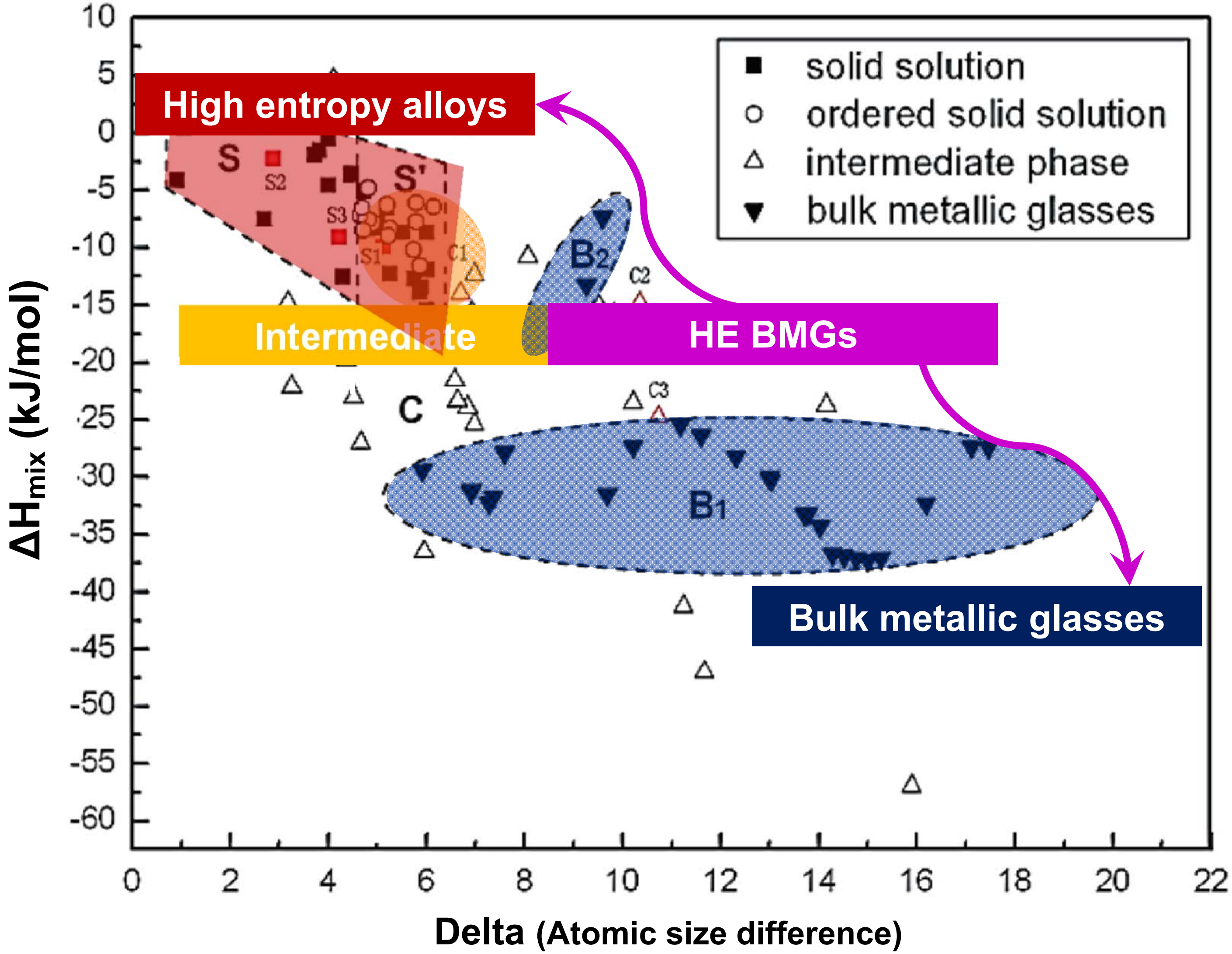

# Thanks for your kind attention

### 4C Current Specifications

| | |
|---|---|
| Beamline | 4C SAXS II |
| Strorage ring energy | 3.0 GeV |
| Source | In-vacuum Undulator 20 (IVU 20) |
| Monochromator | DCM Si (111) Crystal |
| Standard energy (Å / keV) | 1.24 / 10.00 |
| Energy resolution (ΔE/E) | $\sim 2 \times 10^{-4}$ |
| Energy range (keV) | 8 ~ 20 |
| Flux at CCD (ph/s/0.1%BW) | $2 \times 10^{13}$ |
| Beam size at CCD (㎛) | 23 (V) × 300(H) |
| Mirror | Vertical focusing toroidal, rhodium coated |
| Sample-to-detector distance (m) | 0.2 ~ 5.0 |
| Observable minimum angle(°) | 0.00128° (400 nm @ 10 keV) |
| Observable resolution (nm) | 0.3 |
| Detector | Rayonix 2D SX165 |
| Experimental methods | WAXS & SAXS (Bulk, Solution, Powder, Sol-gel, etc) |